Substoichiometric Binding of Taxol Suppresses Microtubule Dynamics†

W. Brent Derry, Leslie Wilson, and Mary Ann Jordan*

Division of Molecular, Cellular, and Developmental Biology, Department of Biological Sciences, University of California—Santa Barbara, Santa Barbara, California 93106

Received September 6, 1994; Revised Manuscript Received November 10, 1994®

ABSTRACT: We have measured the effects of taxol (10 nM to 1 μM) on the growing and shortening dynamics at the ends of individual bovine brain microtubules *in vitro* and have correlated the effects both with the stoichiometry of taxol binding to tubulin in microtubules and with the changes in the microtubule polymer mass. The results indicate that taxol suppresses microtubule dynamic instability differently depending upon the stoichiometry of taxol binding to the microtubules. At the lowest effective concentrations ($\leq$100 nM), substoichiometric binding of taxol to tubulin in microtubules (between 0.001 and 0.01 mol of bound taxol/mol of tubulin in microtubules) potently and selectively suppresses the rate and extent of shortening at plus ends in association with some increase (28% to 60%) in the mass of microtubule polymer. At intermediate taxol concentrations (between 100 nM and 1 μM), the binding of additional taxol molecules to the microtubules (between 0.01 and 0.1 mol of taxol bound/mol of tubulin in microtubules) inhibits both growing and shortening events at both microtubule ends with no additional increase in microtubule polymer mass. At high taxol concentrations and high taxol binding stoichiometries ($\geq$1 μM taxol and $\geq$0.1 mol of taxol bound/mol of tubulin in microtubules), microtubule mass increases sharply and dynamics is almost completely suppressed. The data support the hypothesis that binding of a molecule of taxol to a tubulin subunit in microtubules induces a conformational change in that subunit that strongly reduces its ability to dissociate when the subunit becomes exposed at the microtubule end.

Taxol is an important new cancer chemotherapeutic agent that has been approved for use in refractory ovarian cancer and shows activity against melanoma and breast and lung cancers (McGuire et al., 1989; Holmes et al., 1991; Murphy et al., 1993; Einzig et al., 1991). It is a potent inhibitor of eukaryotic cell proliferation that blocks cell cycle progression at mitosis (Fuchs & Johnson, 1978; Schiff & Horwitz, 1980). Taxol appears to inhibit cell proliferation by an action on microtubules (Schiff & Horwitz, 1980; Jordan et al., 1993; Wilson & Jordan, 1994; Jordan & Wilson, 1995), but the precise molecular and cellular mechanisms are not completely understood.

Microtubules are protein polymers composed of dimeric tubulin subunits arranged head-to-tail in protofilaments, forming the walls of the microtubule (Hyams & Lloyd, 1994). The two ends of each microtubule, termed the plus and minus ends, are structurally and kinetically distinct. During the addition of tubulin to the microtubule ends, the energy provided by hydrolysis of tubulin-liganded GTP[1] to GDP results in two unusual dynamic behaviors termed dynamic instability and treadmilling. Dynamic instability is a stochastic interconversion of the microtubule end between phases of growing and shortening (Mitchison & Kirschner, 1984a,b), which is thought to result from the gain and loss of a stabilizing cap of GTP- or GDP-P_i-liganded tubulin at the microtubule end. Treadmilling or flux is the net growing of a microtubule at one end and the net shortening at the opposite end at polymer mass steady state (Margolis & Wilson, 1978). Treadmilling appears to be a consequence of the inequality of the balance of the association and dissociation rate constants for tubulin at the two microtubule ends.

Taxol reversibly binds to microtubules *in vitro* with a maximum stoichiometry of approximately 1 mol of taxol/mol of tubulin in microtubules and apparently does not bind to free tubulin (Parness & Horwitz, 1981; Diaz et al., 1993). At concentrations that are stoichiometric or near-stoichiometric with respect to the concentrations of tubulin present in solution, taxol strongly stimulates the rate and extent of microtubule polymerization and reduces the concentration of soluble tubulin (Schiff et al., 1979; Kumar, 1981; Howard & Timasheff, 1988). The increased polymer mass is associated with a large taxol-associated linkage free energy contribution (Howard & Timasheff, 1988; Diaz et al., 1993). In addition to stimulating microtubule polymerization, taxol also inhibits tubulin exchange at microtubule ends and treadmilling at polymer mass steady state (Caplow & Zeeberg, 1982; Wilson et al., 1985). Furthermore, at taxol concentrations that result in the approximate stoichiometric binding of taxol to tubulin in microtubules, taxol reduces the flexural rigidity of microtubules (Dye et al., 1993; Venier et al., 1994), and it reduces the protofilament numbers in individual microtubules from approximately 13 to 12 (Andreu et al., 1992). These data indicate that the binding of stoichiometric quantities of taxol to microtubule surfaces induces a conformational change in the tubulin that increases the surface binding contacts between tubulin subunits in the polymer.

In cells, high concentrations of taxol increase microtubule polymer mass and also induce the extensive formation of

† Supported by USPHS Grant CA57291 from the National Cancer Institute. A preliminary account of this work was published in abstract form (Derry et al., 1993).

® Abstract published in *Advance ACS Abstracts,* February 1, 1995.

[1] Abbreviations: DIC, differential interference contrast; EGTA, [ethylenebis(oxyethylenenitrilo)]tetraacetic acid; GTP, guanosine 5′-triphosphate; MAPs, microtubule-associated proteins; PC-tubulin, phosphocellulose-purified tubulin; PEM, 100 mM PIPES, 1 mM EGTA, and 1 mM $MgSO_4$, pH 6.9; PIPES, 1,4-piperazinediethanesulfonic acid.

0006-2960/95/0434-2203$09.00/0

microtubule bundles (Schiff & Horwitz, 1980; De Brabander et al., 1981; Rowinsky et al., 1988; Jordan et al., 1993). Enhanced microtubule polymerization and bundling of microtubules have been suggested to be responsible for the antitumor activity of the drug. However, in previous work we found that low (nanomolar) concentrations of taxol inhibit mitosis in HeLa cells without significantly increasing the microtubule polymer mass (Jordan et al., 1993). Mitotic inhibition by low concentrations of taxol is associated with an altered organization of mitotic spindles that is strikingly similar to that induced by the vinca alkaloids and several other antimitotic drugs known to suppress microtubule dynamics without altering the mass of the microtubules (Jordan et al., 1991, 1992; Toso et al., 1993), leading to the suggestion that, at its lowest effective concentrations, taxol appears to block mitosis by kinetically stabilizing the dynamics of spindle microtubules and not by changing the mass of polymerized microtubules (Jordan et al., 1993).

In the present study we have analyzed the effects of taxol over a wide range of concentrations (10 nM to 10 μM) on growing and shortening dynamics at the ends of individual bovine brain microtubules *in vitro* by video microscopy. We have correlated the actions of the drug on individual dynamic parameters with the stoichiometry of taxol binding to the microtubules and with the changes induced in microtubule mass. The results indicate that taxol suppresses microtubule dynamics differently, depending upon the stoichiometry of taxol binding to the microtubules. At the lowest effective concentrations ($\leq$100 nM), substoichiometric binding of taxol to microtubules (0.001−0.01 mol of taxol/mol of tubulin in microtubules) selectively suppresses the shortening rates at microtubule plus ends. At high taxol binding stoichiometries ($\geq$0.1 mol of taxol/mol of tubulin), microtubule mass increases sharply and dynamics are almost completely suppressed.

MATERIALS AND METHODS

Purification of Tubulin and Flagellar Axonemal "Seeds". Bovine brain microtubule protein (tubulin plus microtubule-associated proteins) was purified by three cycles of warm polymerization and cold depolymerization *in vitro* (Farrell & Wilson, 1984). Tubulin was purified from the microtubule protein by phosphocellulose chromatography (PC-tubulin) (Mitchison & Kirschner, 1984b). PC-tubulin was concentrated to 3 mg/mL in 100 mM PIPES (1,4-piperazinediethanesulfonic acid), 1 mM EGTA, and 1 mM $MgSO_4$ (pH 6.9) at 25 °C (PEM), drop-frozen in liquid nitrogen, and stored at −70 °C. All experiments were performed in PEM except for a small number of dynamics experiments that were performed, as noted in the text, in the presence of high Mg^{2+} concentrations and low PIPES concentrations to obtain more rapid dynamics (50 mM PIPES, 5 mM $MgSO_4$, and 1 mM EGTA, pH 6.9). On the day of an experiment, PC-tubulin was thawed at room temperature and centrifuged (48000*g*, 4 °C, 15 min, Sorvall RC 5B, SS-34 rotor) to remove any aggregated and/or denatured tubulin; the supernatant was used in all experiments. Axoneme "seeds" were prepared from sea urchin sperm (*Strongylocentrotus purpuratus*) (Toso et al., 1993). All protein concentrations were determined (Bradford, 1976) with bovine serum albumin as the standard.

Video Microscopy. Growing and shortening dynamics of individual microtubules were visualized at 30 °C by video-enhanced differential interference contrast (DIC) microscopy. PC-tubulin (17 μM in PEM) was assembled at the ends of axoneme seeds in the presence of 1 mM GTP. At polymer mass steady state (approximately 30 min after the initiation of polymerization, determined by turbidimetry at 350 nm), taxol (NSC125973, a gift from the National Cancer Institute) dissolved in methanol was added to the microtubule suspension, and incubation was continued for an additional 25 min. The methanol concentration was $\leq$1% (v/v) in all experiments, which did not detectably affect microtubule dynamics. Samples (2 μL volumes) were prepared for video microscopy (Toso et al., 1993). Dynamics were analyzed using a Zeiss IM 35 microscope equipped with a Zeiss Planapo 63X 1.4-NA oil immersion objective, a temperature-controlled stage, and a light scrambler (Optiquip 770) with either a 100 W mercury arc lamp or a 150 W halogen lamp. Images were captured in real time using a Hamamatsu C2400 (Newvicon) video camera and recorded on a JVC HRs5800u super VHS video cassette recorder.

Microtubule lengths were measured at 15 s intervals using an IBM AT personal computer equipped with a Targa-M8 frame grabber (Tru-vision) and JAVA video analysis software (Jandel Scientific). We considered the change in length at each 15 s interval to represent either a growing, a shortening, or an attenuation event. Thus, with the method used in this work, growing and shortening events that may have occurred but were too short (0.2 μm) to be detected during a 15 s interval were scored as attenuation events. Between 10 and 18 microtubules were used, and a minimum of 400 individual measurements was made for each experimental condition for analysis of the dynamics of the control and taxol-treated microtubules (except that 80 measurements were made of 4 microtubules treated with 1 μM taxol). Growing and shortening rates were calculated as described previously (Toso et al., 1993). Under the conditions used, microtubule growth at one end of a seed was typically twice as long as growth at the opposite end, and such microtubules were considered to be growing at the plus ends.

Calculation of Transition Frequencies. A "catastrophe" (Walker et al., 1988) was considered to be any shortening of 0.2 μm or greater in a 15 s interval. The catastrophe frequency (number of catastrophes per unit of time) was calculated as the number of shortening events divided by the total time spent growing plus the total time in the attenuated state. A "rescue" (Walker et al., 1988) was considered to be any reversal of shortening. The rescue frequency was calculated as the total number of shortening events that did not extend to the seed divided by the total time spent shortening (Kowalski & Williams, 1993).

Determination of Microtubule Polymer Mass. Microtubules (17 μM total tubulin) were polymerized onto axonemal seeds as described earlier. Taxol was added to the microtubule suspensions at polymer mass steady state (approximately 30 min after the initiation of polymerization, determined by turbidimetry at 350 nm). After an additional 25 min of incubation, aliquots of the suspension (100 μL) were pipeted into Beckman microfuge tubes (5 × 20 mm) and centrifuged (160000*g*, 15 min, 30 °C, Beckman LS-50, SW 50.1 rotor). Supernatants were aspirated, and the microtubule pellets were solubilized in 50 μL of 0.2 M NaOH ($\geq$2 h at 25 °C). Protein concentrations were determined in both supernatant and pellet fractions.

Binding of [^{3}H]Taxol to Microtubules. Binding of taxol to microtubules was measured by a sedimentation assay. Stock solutions of [^{3}H]taxol were prepared by diluting [^{3}H]-taxol (specific activity 19.3 Ci/mmol, obtained from Drs. R. Haugwitz, National Cancer Institute, and J. A. Kepler, Research Triangle Institute, Research Triangle Park, NC) with unlabeled taxol such that the final specific activities ranged from 3×10^{-4} to 19.3 Ci/mmol. Microtubules (17 μM total tubulin) were polymerized onto axonemal seeds as described earlier. Taxol was added to the microtubule suspensions at steady state (approximately 30 min after the initiation of polymerization, determined by light scattering at 350 nm). After an additional 25 min of incubation, 100 μL volumes of the microtubule suspension were layered onto 450 μL of 50% sucrose in PEM at 30 °C and centrifuged (160000*g*, 90 min, 30 °C, Beckman LS-50, SW50.1 rotor) in Beckman microfuge tubes (5 × 41 mm). Supernatants were aspirated, and the cushions were washed twice with deionized water followed by underlayering with 70% sucrose in PEM, which served to displace the 50% sucrose solution and any remaining unbound taxol from the pellet. The remaining sucrose was aspirated, and the pellets were washed with a small volume of 70% sucrose in PEM. Pellets were resuspended in 50 μL of 0.2 N NaOH and incubated for 12 h at room temperature to solubilize the microtubules. Pelleted protein was quantitated, and bound taxol was determined by liquid scintillation spectrometry. Taxol binding was expressed as the number of taxol molecules bound per number of tubulin dimers (M_r = 100 000) in the microtubules.

RESULTS

Effects of Taxol on Microtubule Dynamic Instability

When MAP-depleted tubulin was polymerized in PEM onto axonemal seeds, microtubule formation was observed at both ends of the seeds. However, growth occurred predominantly at the plus ends. The microtubules at polymer mass steady state displayed episodes of growing and shortening characteristic of dynamic instability (Mitchison & Kirschner, 1984b; Horio & Hotani, 1986; Walker et al., 1988; Gildersleeve et al., 1992; Toso et al., 1993); examples of the changes in microtubule length are illustrated in Figure 1A. Microtubules shortened rapidly, grew slowly, and sometimes persisted in an attenuated state in which no growing or shortening was detected (≤0.2 μm in 15 s; see Materials and Methods). The suppressive effects of 25 and 50 nM taxol on microtubule dynamics are illustrated in Figure 1B and 1C, respectively. The effects of taxol (10 nM to 1 μM) on the parameters of dynamic instability are shown quantitatively in Figures 2–4 and Table 1.

Suppression of Shortening Rates at Microtubule Plus Ends. Plus ends of control microtubules shortened at a mean rate of 153 dimers s^{-1} (5.4 μm min^{-1}) (Table 1) and displayed a wide range of shortening rates, from a maximum of 1500 dimers s^{-1} to the minimum detectable of 24 dimers s^{-1}. The plus ends of microtubules grew at a mean rate of 83 dimers s^{-1} (3.0 μm min^{-1}) (Table 1) and also displayed a range of growing rates, from a maximum of 310 dimers s^{-1} to the minimum of 24 dimers s^{-1}. The effects of taxol (10 nM to 1 μM) on the growing and shortening rates are shown in Table 1 and Figure 2. Taxol suppressed the rate of microtubule shortening at a concentration as low as 10 nM.

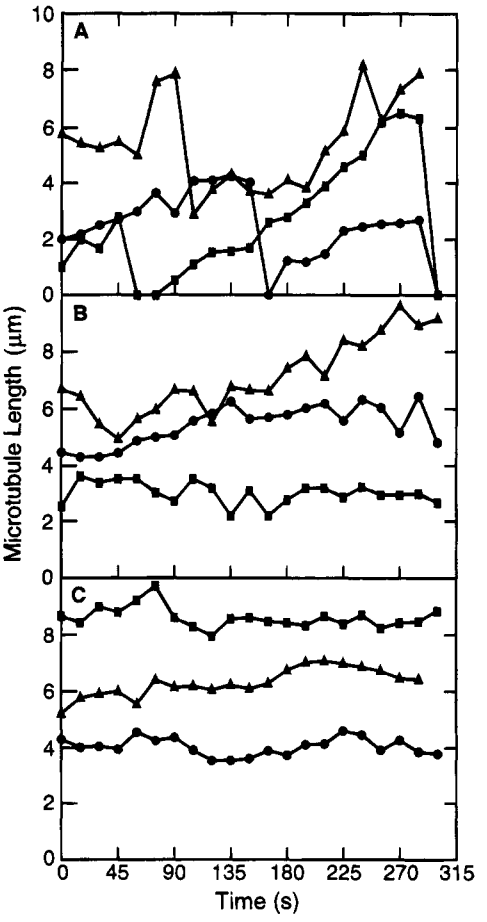

FIGURE 1: Growing and shortening of microtubules at their plus ends in the absence and presence of taxol. Dynamics were analyzed as described in Materials and Methods. Each line represents a single microtubule, and each data point represents the length of the microtubule from its plus end to the nucleating axoneme: A, controls; B, 25 nM taxol; C, 50 nM taxol.

At this concentration, the mean shortening rate at plus ends was 135 dimers s^{-1} (4.8 μm min^{-1}), which is 12% slower than in the absence of taxol. The degree of suppression increased gradually with increasing concentrations of taxol over a 100-fold taxol concentration range.

Low concentrations of taxol also significantly decreased the variability of the shortening rates and prevented the occurrence of all rapid shortening events. For example, at 50 nM taxol the mean shortening rate was decreased by 32%, whereas the maximum shortening rate was decreased by 77% (345 dimers s^{-1} at 50 nM taxol as compared with 1500 dimers s^{-1} in controls) and the standard deviation of the shortening rates (a statistical estimate of the variability) was decreased by 57% (Table 1). Kinetic suppression of microtubule shortening rates at 50 nM taxol was statistically significant compared with control rates (*t*-test, $p \leq 0.05$). Low concentrations of taxol (≤50 nM) did not detectably affect the growing rate (Figure 2, Table 1).

Additional evidence that the shortening rates were more sensitive to taxol than the growing rates was obtained using a buffer consisting of 50 mM PIPES, 1 mM EGTA, and 5 mM Mg^{2+} (pH 6.9), rather than PEM. In the presence of this buffer, the mean shortening rate of control microtubules was considerably higher (250 dimers s^{-1}) than that in the standard PEM buffer (150 dimers s^{-1}). In this buffer system, 50 nM taxol induced a 76% decrease in the mean shortening

Table 1: Effects of Taxol on Kinetic Parameters at Microtubule Ends[a]

[taxol] (μM)	growing rate (dimers/s)	shortening rate (dimers/s)	transitions				
			catastrophe (events/s)	rescue (events/s)	catastrophe (events/μm)	rescue (events/μm)	unrescued catastrophes (%)
0	83 ± 53	153 ± 190	0.02	0.05	0.8	1.1	46
0.01	80 ± 60	135 ± 145	0.02	0.03	0.9	1.1	50
0.025	66 ± 49	104 ± 114	0.02	0.02	1.3	1.3	36
0.05	87 ± 61	104 ± 82	0.03	0.04	1.0	1.3	22
0.1	57 ± 31	59 ± 40	0.02	0.03	1.8	2.1	12
0.5	63 ± 37	62 ± 28	0.06	0.03	1.5	2.2	0
1	31 ± 3	28 ± 4					

[a] Growing and shortening rates are the mean ± one standard deviation. Transition frequencies (*i.e.*, events/s) were calculated according to Walker et al. (1988), but were modified to include transitions into and out of attenuation. Catastrophes/s were calculated as the number of shortening events greater than 0.2 μm divided by the total time spent in growing plus attenuation, while rescues/s were calculated as the number of transitions out of shortening into growth or attenuation divided by the total time spent shortening. Transitions per unit length were calculated according to Kowalski and Williams (1993). Catastrophes/μm were calculated as the total number of shortening events greater than 0.2 μm divided by the total length grown, and rescues/μm were calculated as the total number of transitions from shortening to growing or attenuation divided by the total length shortened. Unrescued catastrophes were calculated as the total number of catastrophic depolymerizations to the nucleating seed divided by the total number of catastrophe events. At 1 μM taxol there was an insufficient number of catastrophes and an insufficient length of microtubule growth to obtain meaningful transition frequency data.

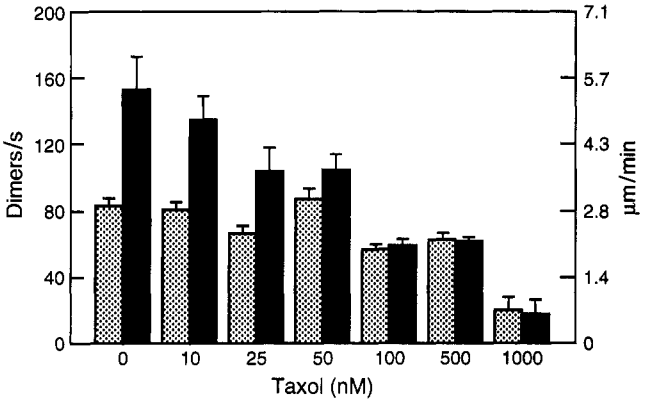

FIGURE 2: Effects of taxol on growing and shortening rates. Mean growing rates (dotted bars) and shortening rates (solid bars) are presented in dimers second^{-1} and micrometers minute^{-1}. The number of microtubules analyzed at each taxol conncentration was as follows: control (0 taxol), 18; 10 nM, 15; 25 nM, 11; 50 nM, 11; 100 nM, 17; 500 nM, 10; 1000 nM, 4. Error bars represent the standard error of the mean.

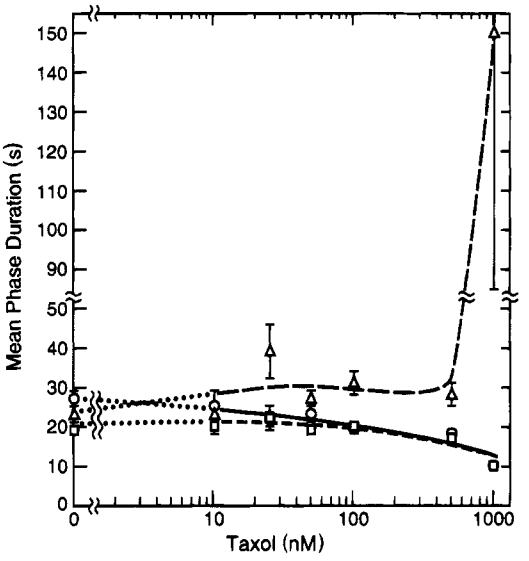

FIGURE 3: Effects of taxol on the mean growing duration (circles), mean shortening duration (squares), and mean attenuation duration (triangles) (Materials and Methods). Error bars represent the standard error of the mean.

rate without detectably affecting the growing rate (data not shown).

At taxol concentrations below 100 nM, there were no detectable effects on minus end microtubule dynamics. At taxol concentrations ≥100 nM, microtubules at the plus and minus ends of the seeds became indistinguishable; the microtubules grew to similar lengths at both ends of the seeds, and their growing and shortening rates were similar. Data at taxol concentrations ≥100 nM, therefore, represent a mixture of plus ends and minus ends. In this taxol concentration range, both growing and shortening rates were suppressed in a concentration-dependent manner, and the mean shortening rates were similar to the mean growing rates. For example, at 100 nM taxol, shortening rates were 59 dimers s^{-1} (2.1 μm min^{-1}) and growing rates were 57 dimers s^{-1} (2.0 μm min^{-1}) (Table 1). At 1 μM taxol, the shortening and growing rates were reduced to such a degree (28 and 31 dimers s^{-1}, respectively) that they were barely measurable and the microtubules were in the attenuated state 90% of the time (see Figure 4C). Thus, in contrast to the effects of taxol at low concentrations, at concentrations ≥100 nM, *both* growing and shortening rates were suppressed and microtubule ends became indistinguishable.

Effects of Taxol on the Durations of the Growing, Shortening, and Attenuation Phases and on the Frequency of Transitions between the Phases. In contrast to the strong action of taxol on the growing and shortening rates, taxol affected the durations of the growing, shortening, and attenuation phases only to a very small degree over a broad taxol concentration range (10−500 nM taxol, Figure 3). Even at a taxol concentration as high as 500 nM, the mean duration of the shortening events was decreased by only 11%, the mean duration of the growing events was decreased by 33%, and the mean duration of the attenuation events was increased by 22%. However, as the taxol concentration was increased from 500 to 1000 nM, the mean duration of the attenuation events increased enormously (by 650%).

The effects of taxol on the frequency of transition among phases of growing, shortening, and attenuation were calculated as events per unit of time (Materials and Methods) (Table 1). Importantly, taxol had no effect on either the catastrophe frequency or the rescue frequency at taxol concentrations ≤500 nM. In contrast, at 1000 nM taxol,

catastrophes (and therefore also rescues) became extremely rare.

However, when we analyzed the proportions of shortening events that led to complete depolymerization of the microtubule or to a rescue, we found that taxol had a profound effect. With control microtubules, 50% of the shortening events of at least 0.5 μm of microtubule length ultimately resulted in complete microtubule depolymerization, and taxol greatly decreased the proportion of such shortening events. For example, at 100 nM taxol, only 10% of such shortening events led to complete depolymerization, and at ≥500 nM taxol, none of the shortening events resulted in complete depolymerization (*i.e.*, all depolymerization events were rescued).

Another meaningful way to characterize the transitions is to analyze the number of rescues per length shortened and the number of catastrophes per length grown (Kowalski & Williams, 1993). Both parameters were increased by taxol (Table 1). For example, 500 nM taxol doubled both the number of rescues per length shortened and the number of catastrophes per length grown (rescues per micrometer of length shortened: 2.2 with 500 nM taxol compared with 1.1 in controls; catastrophes per micrometer of length grown: 1.5 with 500 nM taxol compared with 0.8 in controls).

Taxol affected the percentage of total time that the microtubules spent growing, shortening, and in the attenuated state in an interesting way. In the absence of taxol, microtubule plus ends spent approximately 43% of the total time growing, 26% of the time shortening, and 31% of the time in an attenuated state. As the concentration of taxol was increased between 10 and 500 nM, the fraction of time that the microtubules spent growing decreased only slightly, to approximately 34% (Figure 4A), the percentage of time the microtubules spent shortening remained at approximately 26% (Figure 4B), and the fraction of time the microtubules spent in the attenuated state increased only slightly, to approximately 40% (Figure 4C). However, as the concentration of taxol was raised from 500 to 1000 nM, the effects of the drug on the percentage of time in each phase became marked. At 1000 nM taxol, microtubules spent 90% of the time in the attenuated state, but only 7% of the time growing and 3% of the time shortening.

Effects of Taxol on the Microtubule Polymer Mass

The addition of taxol to microtubule suspensions increased the steady-state polymer mass in a complex manner (Figure 5). The lowest concentrations of taxol studied (10−50 nM) induced some increase in polymer mass; for example, at 50 nM taxol, polymer mass was increased 1.6-fold over controls. Between 50 and 500 nM taxol, there was no further increase in polymer mass. However, at taxol concentrations ≥1 μM, polymer mass increased greatly. For example, at 1 μM taxol, polymer mass increased 1.9-fold over controls, whereas at 20 μM taxol, polymer mass increased 2.6-fold over controls.

Binding of Taxol to Microtubules and Correlation of Binding Stoichiometry with the Extent of Shortening

In order to elucidate the mechanism by which taxol suppresses microtubule dynamics, we determined the stoichiometry of [^{3}H]taxol binding to tubulin in microtubules over the range of taxol concentrations used in the foregoing experiments, using similar experimental conditions. The

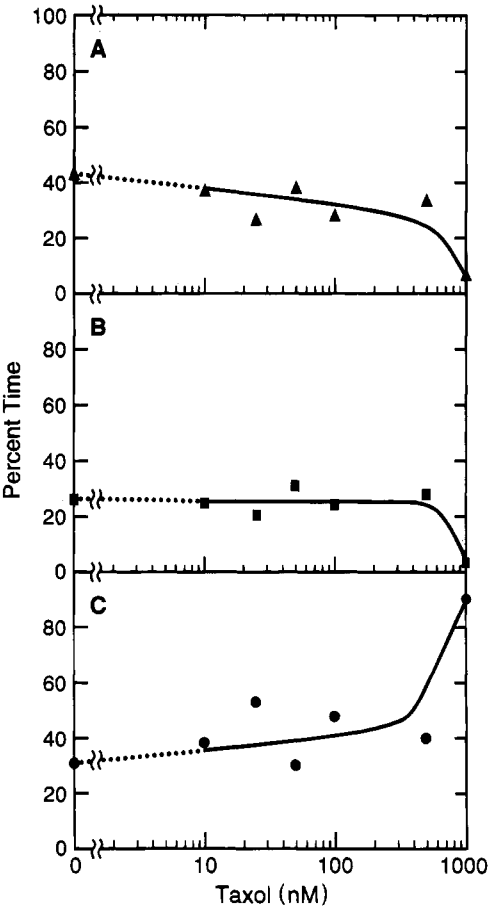

FIGURE 4: Effects of taxol on the percentage of total time microtubules spent growing (A), shortening (B), or in the attenuation phase (C).

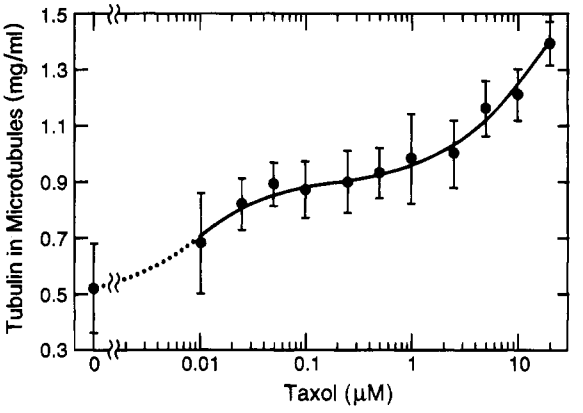

FIGURE 5: Effects of taxol on the mass of microtubule polymer. Total tubulin concentration was 17 μM. Data points represent the mean of four independent experiments; error bars are the standard deviation.

stoichiometry of taxol binding to tubulin in steady-state microtubules as a function of taxol concentration is presented in Table 2 and Figure 6. The binding of taxol to microtubules followed a complex relationship with the logarithm of taxol concentration (Figure 6). In the presence of 10 nM taxol, 1 taxol molecule was bound for every 688 tubulin dimers (stoichiometry of 0.0015, Table 2), while at 50 nM taxol, 1 taxol molecule was bound for every 150 tubulin dimers (stoichiometry of 0.0066). At 5 μM taxol, binding was saturated at a stoichiometry of 1 taxol molecule per tubulin dimer in microtubules, in agreement with previous reports (Parness & Horwitz, 1981; Diaz & Andreu, 1993).

Table 2: Stoichiometry of Taxol Binding to Microtubules[a]

[taxol] (μM)	taxol bound per tubulin dimer in microtubules (mol/mol)
0	
0.01	0.0015 ± 0.0003
0.025	0.0037 ± 0.0008
0.05	0.0066 ± 0.0014
0.10	0.014 ± 0.007
0.25	0.028 ± 0.006
0.50	0.051 ± 0.011
0.75	0.072 ± 0.009
1.0	0.12 ± 0.04
2.5	0.54 ± 0.10
5.0	1.15 ± 0.31
10.0	0.91 ± 0.07
20.0	1.16 ± 0.13

[a] Data are the mean of four separate experiments ± one standard deviation.

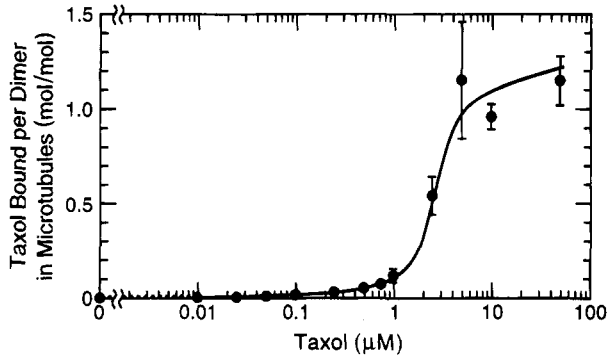

FIGURE 6: Isotherm of taxol binding to microtubules. Portions of a microtubule suspension at steady state (17 μM tubulin) were incubated with [^{3}H]taxol at concentrations between 0.01 and 50 μM for 30 min at 30 °C. [^{3}H]Taxol and protein were determined in microtubule pellets after centrifugation through 50% sucrose cushions (Materials and Methods). Bound taxol is expressed as the molar ratio of taxol bound per tubulin dimer in microtubules.

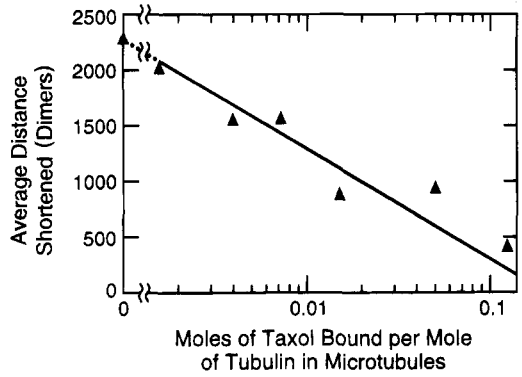

FIGURE 7: Binding of taxol to microtubules in relation to the average distance shortened during a shortening event.

The relationship between the extent of shortening and the number of taxol molecules bound to the microtubules is shown in Figure 7. The extent of shortening decreased with increasing stoichiometry of bound taxol. In the absence of taxol, microtubules shortened by an average distance of 2295 dimers (1.4 μm) during a shortening event. At 25 nM taxol, a concentration that resulted in a stoichiometry of only 0.004 mol of taxol/mol of tubulin in microtubules, the average distance shortened was reduced to 1550 dimers (0.9 μm). Half-maximal inhibition of the average distance shortened occurred at a taxol binding stoichiometry of 0.017 mol of taxol bound/mol of tubulin in microtubules. Thus, small numbers of taxol molecules distributed along the microtubule surface, considerably fewer than the number of tubulin molecules, strongly reduced the extent of microtubule shortening.

DISCUSSION

We have analyzed the effects of taxol over a wide range of concentrations (10 nM to 1 μM) on the growing and shortening dynamics at the ends of individual microtubules and have correlated the effects with the stoichiometry of taxol binding to the microtubules. The effects of taxol varied both qualitatively and quantitatively with the stoichiometry of taxol binding. Kinetic suppression of the shortening rates at the plus ends was the most striking effect of taxol binding at low stoichiometries (between 0.001 and 0.014 mol of taxol/mol of tubulin in microtubules, taxol concentrations between 10 and 100 nM; Table 2, Figure 2). Suppression of the shortening rates was accompanied by a reduction in the variability of the shortening rates and a reduction in the average distance that the microtubules shortened during a shortening event (Figure 7). Neither the growing rates at the plus ends nor the shortening or growing rates at the minus ends were detectably affected. In this concentration range, there was a 28− 60% increase in the mass of microtubule polymer as compared with controls (Figure 5).

Between 100 nM and 1 μM taxol, binding stoichiometry increased from 0.014 to 0.115 mol of taxol bound/mol of tubulin in microtubules (Table 2); however, there was little additional change in the mass of microtubule polymer (Figure 5). In this binding range, taxol suppressed the growing rates in addition to suppressing the shortening rates, and it increased the percentage of time that the microtubules spent in the attenuated state (Figure 4C). Microtubules at both plus and minus ends of axonemal seeds grew to similar lengths, and the shortening and growing rates were inhibited to such an extent that the plus and minus ends were indistinguishable.

At taxol concentrations greater than 1 μM, taxol binding to microtubules approached saturation (attaining a stoichiometry of 1 mol taxol bound/mol of tubulin in microtubules at 5 μM taxol; Figure 6, Table 2). Microtubules spent ≥90% of the time in the attenuated state, and microtubule dynamics was nearly completely shut down (Figures 2−4). The microtubule polymer mass increased sharply. At 20 μM taxol, the soluble tubulin was undetectable by the Bradford assay (Figure 5).

Effects of Taxol on Microtubule Dynamic Instability

Effects of Taxol on the Rate and Extent of Shortening. The most potent action of taxol on microtubule dynamics was the suppression of the rate and extent of shortening. Suppression of shortening resulted from the binding of very few taxol molecules to the microtubules. Suppression of the extent of shortening increased linearly with the logarithm of the taxol binding stoichiometry (Figure 7). The binding of a few taxol molecules to the microtubules sharply decreased the average distance shortened during a shortening event. However, the binding of each additional taxol molecule had a diminishing additional effect on the average distance shortened. For example, in the absence of taxol, microtubules shortened 2300 dimers during an average shortening event. The average distance shortened was

reduced by 33% to 1550 dimers per event by the binding of only a few taxol molecules to the microtubule (stoichiometry of 0.004). An equivalent further reduction in the average distance shortened (by 67%, to 770 dimers per event) required a nearly 10-fold increase in taxol binding to a stoichiometry of 0.035. Complete suppression of the shortening distance required a saturating density of taxol on the microtubule surface (stoichiometry of ~1 mol of taxol bound/mol of tubulin).

If taxol were bound uniformly and with a single affinity along the surface of the microtubule, doubling the taxol binding stoichiometry would be expected to halve the distance shortened during an average shortening event. The observation that as the taxol binding stoichiometry increased the additional taxol molecules did not reduce shortening as strongly as the first bound taxol molecules suggests that the binding is nonuniform or of more than one affinity. One possible explanation is that taxol may bind with lower affinity to the microtubule ends than to the internal core regions of the microtubule (discussed further in the following).

Effects of Taxol on Transition Frequencies. Neither the catastrophe frequency nor the rescue frequency was altered over a broad range of taxol binding stoichiometries (between 0.001 and 0.05 mol of taxol bound/mol of tubulin in microtubules, taxol concentrations of 10−500 nM; Table 1). Even when the rates of growing and shortening were markedly suppressed, microtubules were still able to undergo normal transitions into either the growing or the shortening phase. These results indicate that taxol may not directly alter the rate of gain or loss of the stabilizing GTP or GDP-P_i cap at microtubule ends. However, the frequency of transition into the shortening phase decreased sharply to near zero at higher binding stoichiometries (≥0.1 mol of bound taxol/mol of tubulin in microtubules, ≥1 μM taxol). Inhibition of the frequency of transition to shortening by taxol at high binding stoichiometries is probably a result of suppression of the length changes at microtubule ends to such a strong degree that the length changes become undetectable (*i.e.*, the microtubules are in the attenuated state).

We calculated the effects of bound taxol on the frequency of unrescued catastrophes and found that the percentage of time that microtubules depolymerized entirely to the seeds decreased from 46% in controls to 0% at a taxol binding stoichiometry of 0.05 (500 nM taxol). Exposure of taxol-liganded tubulin at microtubule ends during shortening may favor rescue by increasing the affinity of the microtubule end for the addition of GTP−tubulin (discussed further in the following).

The Mechanism of Action of Taxol

As indicated earlier (introduction), the binding of stoichiometric quantities of taxol to tubulin in microtubules strongly reduces the free energy of polymerization and modifies the structure of the microtubule in ways that suggest that taxol-induced conformational changes in the tubulin result in increased subunit−subunit contact sites. Thus, it seems highly plausible that the binding of a single molecule of taxol to its tubulin binding site in an otherwise normal region of the microtubule surface might induce a similar conformational change. The observed suppression of the rate and extent of microtubule shortening is very sensitive to the binding of a few taxol molecules, but as the binding stoichiometry increases, the extent to which taxol further inhibits this process becomes less pronounced. A simple and attractive model to account for this effect would predict that microtubule depolymerization occurs normally until such a taxol-liganded tubulin subunit is reached, upon which shortening stops due to the substantially higher affinity of the taxol-liganded tubulin molecule for the polymer than for unliganded tubulin subunits. Shortening can resume upon dissociation of the taxol. Alternatively, shortening might resume upon the eventual dissociation of the taxol−tubulin complex. The less potent suppression of shortening events observed at higher taxol binding stoichiometries may be partially attributable to the limit of resolution of our system (0.2 μm; see Materials and Methods). Otherwise, the nonlinear effects of taxol on the suppression of shortening rates and distances may arise from the occupation of high-affinity binding sites at low concentrations.

The theory of linked functions predicts that when a ligand is involved in a conformational change or in a polymerization process the equilibrium is displaced toward the species of greater binding (Wyman, 1964; Diaz et al., 1993). The microtubule, as opposed to soluble tubulin, is the species of greater binding. Thus, from the theory of linked functions, bound taxol would be predicted to decrease the dissociation rate constant for the taxol-liganded tubulin when it is situated at the microtubule end or to increase the association rate constant for the addition of tubulin to the taxol-liganded tubulin situated at the microtubule end. A taxol-induced decrease in the dissociation rate constant has been observed (Caplow & Zeeberg, 1982; Wilson et al., 1985). However, an increase in the association rate constant has not been detected experimentally. One might expect that at low taxol binding stoichiometries an increase in the association rate constant would be detectable only on a microscopic level during the addition of only one or a few new tubulin molecules to taxol-liganded tubulin situated at a microtubule end. One might also expect that an increase in the association rate constant would be nullified after the addition of sufficient unliganded tubulin to the microtubule end and thus would be difficult to detect experimentally.

The binding of small numbers of taxol molecules to microtubules (stoichiometries between 0.001 and 0.007 mol of taxol bound/mol of tubulin in microtubules, 10−50 nM taxol) caused a small but measurable increase in the microtubule polymer mass. The increase in polymer mass at low taxol stoichiometries is probably a consequence of the reduced shortening rates coupled with the absence of effects on the growing rates. Interestingly, the binding of additional taxol molecules to stoichiometries of 0.05 (at 500 nM taxol) resulted in no additional increase in polymer mass. The lack of any further increase in polymer mass in this taxol binding stoichiometry range is surprising and is probably linked in a complex way to the action of taxol on the balance between growing and shortening. Inhibition of the shortening rate and the resultant decrease in the concentration of soluble tubulin would be expected to lead to inhibition of the growing rate, because the growing rate is determined by the association rate constant and the soluble tubulin concentration.

The binding of nearly saturating numbers of taxol molecules (≥0.11 mol of taxol bound/mol of tubulin) at high taxol concentrations (≥1 μM taxol) induced an additional

sharp increase in the polymer mass (Figure 5), suggesting that the mechanism of action of taxol in this range of binding stoichiometries may be altered in some way. One possible explanation, mentioned previously, is that taxol may bind to the internal core regions of the microtubule with higher affinity than it binds near the ends, *i.e.*, that significant binding of taxol to microtubule ends occurs only at relatively high taxol concentrations. Carlier and Pantaloni (1983) have previously suggested that microtubule ends may have a lower affinity for taxol than the cores. These authors found that suprastoichiometric concentrations of taxol (40−90 μM taxol and 15 μM tubulin) were required to block GTP hydrolysis, which is considered to take place at or near the ends of microtubules. In addition, Wilson et al. (1985) found that taxol at concentrations that reduced the tubulin dissociation rate constant and inhibited the rate of treadmilling had little or no effect on the rapid burst of GTP incorporation that occurs at or near the microtubule ends. As the concentration of taxol is raised and the binding sites in the internal core regions of the microtubule become saturated, taxol may bind to a significant number of sites at the microtubule ends and induce conformational changes in tubulin at the ends, which favors tubulin subunit addition to the ends. Thus, at very high taxol binding stoichiometries, the equilibrium between polymer and soluble tubulin shifts sharply in favor of polymer, resulting in a reduction of the concentration of soluble tubulin to undetectable levels.

The Taxol Binding Mechanism

In part because the mass of polymerized microtubules (the receptor) increased with increasing taxol concentrations, determination of a binding constant from the taxol binding data (Figure 6, Table 2) is difficult. In addition, over the range of taxol concentrations used, the free taxol concentration was very low; most of the taxol added was bound to the microtubules. A Scatchard plot (Scatchard, 1949) of the binding data shown in Figure 6 was nonlinear, indicating the possible presence of more than a single affinity class of sites or of negative cooperativity (data not shown). However, rigorous analysis of the binding data was not feasible.

Comparison of Taxol with MAPs and with Vinblastine

Microtubule-associated proteins (MAPs) and taxol both bind along the surface of microtubules and both suppress dynamic instability. In particular, MAPs and taxol both potently suppress the rates and extents of microtubule shortening (Pryer et al., 1993; Kowalski & Williams, 1993; Toso et al., 1993). However, in contrast to taxol, saturating concentrations of MAP2 or tau do not completely suppress shortening, nor do they reduce the frequency of transition into the shortening phase to zero (Pryer et al., 1993; Kowalski & Williams, 1993). Taxol appears to be an especially potent MAP-like molecule that may bind to a natural regulatory site on the microtubule surface.

Taxol and vinblastine both strongly suppress microtubule dynamics at substoichiometric concentrations *in vitro* (Figures 1 and 2 and Table 1; Toso et al., 1993). The effects of the two drugs on dynamics are similar in important ways. Specifically, the binding of small numbers of taxol or vinblastine molecules to microtubules suppresses the rate of microtubule shortening. However, in contrast with taxol, which suppresses microtubule dynamics at low concentrations by binding to the surface of the microtubule, vinblastine suppresses dynamics by binding to a small number of sites at the microtubule ends (Wilson et al., 1982; Jordan & Wilson, 1990).

The two drugs also show important differences in other ways. For example, vinblastine suppresses the growing and shortening rates to the same degree and increases the percentage of time the microtubules spend in an attenuated state at low concentrations, whereas low concentrations of taxol inhibit only the shortening rate. In addition, the suppression of dynamics by vinblastine exhibits a very steep concentration dependence (Toso et al., 1993), while that for taxol is gradual. Specifically, the suppression of dynamics is detected only at concentrations of vinblastine $\geq$500 nM and is maximal at a 2-fold higher concentration (1 μM). In contrast, with taxol the suppression of shortening is detected at concentrations as low as 10 nM, but is maximal only at 100-fold higher concentrations (1 μM).

Relationship between the Suppression of Dynamic Instability by Taxol and Its Antimitotic and Antitumor Activities

We previously found that taxol, like vinblastine, potently blocks mitosis in HeLa cells at the metaphase/anaphase transition with little or no associated change in the mass of microtubule polymer. In addition, both drugs induce a similar concentration-dependent array of mitotic spindle abnormalities (Jordan et al., 1991, 1992, 1993). For example, at low concentrations of either taxol (10 nM) or vinblastine (0.8 nM), the spindles are bipolar, they are shorter than spindles in control cells, and they contain a few chromosomes that are unable to congress to the metaphase plate. At somewhat higher concentrations of either drug, the spindles are predominantly monopolar ball-shaped aggregations of condensed chromosomes. Previously we suggested that the altered spindle organization and the mitotic block induced by both drugs result from the kinetic suppression of spindle microtubule dynamics (Jordan et al., 1993).

However, there are also interesting differences in the actions of taxol and vinblastine on mitosis that may be related to the different specific mechanisms by which the two drugs suppress microtubule dynamics. With vinblastine, the occurrence of spindle abnormalities correlates strictly with mitotic block at the metaphase/anaphase transition. For example, at 0.1 nM vinblastine, the spindles are normal and mitosis proceeds normally, whereas at higher concentrations, *e.g.*, 0.8 nM vinblastine, spindle organization is detectably abnormal and mitosis is blocked (Jordan et al., 1991, 1992). However, taxol induces numerous spindle abnormalities at very low concentrations without causing mitotic block. For example, at 1 nM taxol, 58% of spindles exhibit detectable abnormalities, but mitosis is not blocked and there is no inhibition of proliferation. At low taxol concentrations, progression through metaphase may be slowed but progression to anaphase is not blocked.

The differences in the actions of the two drugs may result from the relationship between the stoichiometry of binding of the two drugs to the microtubules and the degree to which the specific dynamic parameters are suppressed. Binding of only a few molecules of vinblastine to microtubule ends maximally suppresses growing and shortening dynamics at the ends. However, in contrast, taxol at the lowest effective

binding stoichiometries inhibits only the rate and extent of shortening; much higher binding stoichiometries are required to suppress dynamics maximally. The reduction in the rate and extent of microtubule shortening by taxol and the suppression of unrescued catastrophes may impair spindle formation and slow chromosome congression without necessarily inducing a complete metaphase block. Lasting mitotic block and inhibition of cell proliferation by taxol may require that the spindle microtubule dynamics be significantly attenuated, which requires the binding of high numbers of taxol molecules to the microtubules.

In summary, the mechanism of action of taxol appears to be more complex than previously envisioned, and the action of the drug is dependent upon the stoichiometry of its binding to tubulin in the microtubules. At its lowest effective concentrations, the binding of a few molecules of taxol to the microtubule (0.001−0.01 mol of taxol/mol of tubulin in microtubules) potently suppresses the rate and extent of shortening at microtubule plus ends, with some effects on the mass of microtubule polymer. Bound taxol may act in this range of stoichiometries by inhibiting the dissociation rate constant of taxol-liganded tubulin molecules and by transiently increasing the association rate constant for tubulin addition to taxol-liganded tubulin located at the microtubule end. At intermediate taxol binding stoichiometries (0.01−0.1 mol of taxol/mol of tubulin in microtubules), both growing and shortening are inhibited at both microtubule ends with no significant increase in microtubule polymer mass. At high binding stoichiometries (≥0.1 mol of taxol/mol of tubulin in microtubules), almost all soluble tubulin is effectively recruited into the microtubule polymer, and microtubule dynamics becomes completely suppressed by taxol. Similarly, the effects of taxol on cellular microtubule function can be expected to vary significantly with the stoichiometry of taxol binding to microtubules.

ACKNOWLEDGMENT

We thank Mr. Herb Miller for excellent technical assistance and Dr. Dulal Panda, Dr. Kevin Farrell, Dr. Stanley Parsons, Etsuko Tsuchiya, Cynthia Dougherty, Doug Thrower, and Dr. Pete Raimondi for stimulating and helpful discussions.

REFERENCES

Andreu, J. M., Bordas, J., Diaz, J. F., Garcia de Ancos, J., Gil, R., Medrano, F. J., Nogales, E., Pantos, E., & Towns-Andrews, E. (1992) *J. Mol. Biol. 226*, 169−184.

Bradford, M. M. (1976) *Anal. Biochem. 72*, 248−254.

Caplow, M., & Zeeberg, B. (1982) *Eur. J. Biochem. 127*, 319−324.

Carlier, M.-F., & Pantaloni, D. (1983) *Biochemistry 22*, 4814−4822.

De Brabander, M., Geuens, G., Nuydens, R., Willebrords, R., & De Mey, J. (1981) *Proc. Natl. Acad. Sci. U.S.A. 78*, 5608−5612.

Derry, W. B., Wilson, L., & Jordan, M. A. (1993) *Mol. Biol. Cell 4*, 163a.

Diaz, J. F., & Andreu, J. M. (1993) *Biochemistry 32*, 2747−2755.

Diaz, J. F., Menendez, M., & Andreu, J. M. (1993) *Biochemistry 32*, 10067−10077.

Dye, R. B., Fink, S. P., & Williams, R. C., Jr. (1993) *J. Biol. Chem. 268*, 6847−6850.

Einzig, A. I., Hochster, H., Wiernik, P. H., Trump, D. L., Dutcher, J. P., Garowski, E., Sasloff, J., & Smith, T. J. (1991) *Invest. New Drugs 9*, 59−64.

Farrell, K. W., & Wilson, L. (1984) *Biochemistry 23*, 3741−3748.

Fuchs, D. A., & Johnson, R. K. (1978) *Cancer Treat. Rep. 62*, 1219−1222.

Gildersleeve, R. F., Cross, A. R., Cullen, K. E., Fagan, L. P., & Williams, R. C., Jr. (1992) *J. Biol. Chem. 267*, 7995−8006.

Holmes, F. A., Walters, R. S., Theriault, R. L., Forman, A. D., Newton, L. K., Raber, M. N., Buzdar, A. U., Frye, D. K., & Hortobagyi, G. N. (1991) *J. Natl. Cancer Inst. 83*, 1797−1805.

Horio, T., & Hotani, H. (1986) *Nature 321*, 605−607.

Howard, W. D., & Timasheff, S. N. (1988) *J. Biol. Chem. 263*, 1342−1346.

Hyams, J. S., & Lloyd, C. W. (Eds.) (1994) *Microtubules*, Wiley-Liss, Inc., New York.

Jordan, M. A., & Wilson, L. (1990) *Biochemistry 29*, 2730−2739.

Jordan, M. A., & Wilson, L. (1995) in *Taxane Anticancer Agents, Basic Science and Current Status* (Georg, G. I., Chen, T. T., Ojima, I., & Vyas, D. M., Eds.) pp 138−153, American Chemical Society Symposium Series 583, American Chemical Society, Washington, D.C.

Jordan, M. A., Thrower, D., & Wilson, L. (1991) *Cancer Res. 51*, 2212−2222.

Jordan, M. A., Thrower, D., & Wilson, L. (1992) *J. Cell Sci.*, 401−416.

Jordan, M. A., Toso, R. J., Thrower, D., & Wilson, L. (1993) *Proc. Natl. Acad. Sci. U.S.A. 90*, 9552−9556.

Kowalski, R. J., & Williams, R. C., Jr. (1993) *J. Biol. Chem. 268*, 9847−9855.

Kumar, N. (1981) *J. Biol. Chem. 256*, 10435−10441.

Margolis, R. L., & Wilson, L. (1978) *Nature 272*, 450−452.

McGuire, W. P., Rowinsky, E. K., Rosensheim, N. B., Grumbine, F. C., Ettinger, D. S., Armstrong, D. K., & Donehower, R. C. (1989) *Ann. Intern. Med. 111*, 273−279.

Mitchison, T. J., & Kirschner, M. (1984a) *Nature 312*, 232−237.

Mitchison, T. J., & Kirschner, M. (1984b) *Nature 312*, 237−242.

Murphy, W. K., Fossella, F. V., Winn, R. J., Shin, D. M., Hynes, H. E., Gross, H. M., Davilla, E., Leimert, J., Dhingra, H., & Raber, M. N. (1993) *J. Natl. Cancer Inst. 85*, 384−388.

Parness, J., & Horwitz, S. B. (1981) *J. Cell Biol. 91*, 479−487.

Pryer, N. K., Walker, R. A., Skeen, V. P., Bourns, B. D., Soboeiro, M. F., & Salmon, E. D. (1993) *J. Cell Sci. 103*, 965−976.

Rowinsky, E. K., Donehower, R. C., Jones, R. J., & Tucker, R. W. (1988) *Cancer Res. 49*, 4093−4100.

Scatchard, G. (1949) *Ann. N. Y. Acad. Sci. 51*, 660−692.

Schiff, P. B., & Horwitz, S. B. (1980) *Proc. Natl. Acad. Sci. U.S.A. 77*, 1561−1565.

Schiff, P. B., Fant, J., & Horwitz, S. B. (1979) *Nature 277*, 665−667.

Toso, R. J., Jordan, M. A., Farrell, K. W., Matsumoto, B., & Wilson, L. (1993) *Biochemistry 32*, 1285−1293.

Venier, P., Maggs, A. C., Carlier, M.-F., & Pantaloni, D. (1994) *J. Biol. Chem. 269*, 13353−13360.

Walker, R. A., O'Brien, E. T., Pryer, N. K., Soboeiro, M. F., Voter, W. A., Erickson, H., & Salmon, E. D. (1988) *J. Cell Biol. 107*, 1437−1448.

Wilson, L., & Jordan, M. A. (1994) in *Microtubules* (Hyams, J., & Lloyd, C., Eds.) pp 59−84, John Wiley and Sons, Inc., New York.

Wilson, L., Jordan, M. A., Morse, A., & Margolis, R. L. (1982) *J. Mol. Biol. 159*, 129−149.

Wilson, L., Miller, H. P., Farrell, K. W., Snyder, K. B., Thompson, W. C., & Purich, D. L. (1985) *Biochemistry 24*, 5254−5262.

Wyman, J. (1964) *Adv. Protein Chem. 19*, 224−285.

BI942114R